

# THERMAL STRATIFICATION AND CHEMICAL REACTION EFFECTS ON MHD FLOW THROUGH OSCILLATORY VERTICAL PLATE IN A POROUS MEDIUM WITH TEMPERATURE VARIATION AND EXPONENTIAL MASS DIFFUSION

 Digbash Sahu\*,  Rudra Kanta Deka

*Department of Mathematics, Gauhati University, Guwahati, 781014, Assam, India*

*\*Corresponding Author e-mail: [digbashsahu79@gmail.com](mailto:digbashsahu79@gmail.com)*

Received April 1, 2024; revised April 19, 2024; accepted May 5, 2024

This research paper investigates the thermal stratification and chemical reaction effects on MHD Flow through oscillatory vertical plate in a porous medium with temperature variation and exponential mass diffusion. Through the application of the Laplace transform method, the paper derives analytical solutions that precisely depict the physical dynamics of the flow. The investigation utilizes sophisticated mathematical models to scrutinize the complex dynamics between Magnetohydrodynamics (MHD) and convective movements, considering a range of conditions involving temperature fluctuations and exponential rates of mass diffusion. A pivotal finding from this research is the detailed comparison between the outcomes of thermal stratification and those observed in environments lacking such stratification. It is observed that the implementation of stratification within the flow leads to a more rapid achievement of equilibrium or steady-state conditions.

**Keywords:** *MHD flow; Chemical Reaction; Thermal Stratification; Porous Medium; Oscillatory Vertical Plate; Laplace Transform; Matlab*

**PACS:** 44.05.+e, 44.25.+f, 47.11.-j, 47.55.P-, 47.56.+r, 47.65.-d

## 1. INTRODUCTION

The ubiquitous phenomena of thermal stratification in fluid systems result from fluids innate propensity to arrange themselves into discrete temperature strata according to their thermal characteristics. The temperature distribution that is stratified within a fluid medium is a key factor in determining the thermal properties of different natural and artificial settings. Thermal stratification has a significant impact on heat transport, energy efficiency, and environmental dynamics. It is especially common in water bodies, atmospheric conditions, and industrial operations.

This research represents the first of its kind to examine the combined effects of thermal stratification and chemical reaction on the flow around an oscillating vertical plate, building on a foundation established by previous studies in related areas. Initial efforts by [1] and [2] were crucial in developing an understanding of transient free convection flows along vertical flat plates, which was further expanded upon by [3] who looked into unsteady natural convection adjacent to infinitely long vertical plates. Subsequent research broadened the scope of investigation into various facets of this phenomenon. Investigations into transient buoyant flows within stratified fluids were conducted by [4] and [5, 6], while [7] focused on flow dynamics driven by convection in fluids that were stably stratified. The domain of porous media received significant attention as well, with [8] studying unsteady free convection in a porous medium saturated with fluid, and [9] delving into the dynamics of heat and mass transfer through natural convection in such mediums. The role of radiation and magnetic fields in these processes was not overlooked; [10] assessed MHD boundary layer flow over vertical plates with a gradient in temperature, and [11] evaluated MHD free convective mass transfer effects alongside variable suction and the Soret effect. The interaction between chemical reaction and thermal radiation received particular focus in the works of [12] and [13], who explored the influence of chemical reaction on vertical plates subjected to radiation and thermal stratification. The dynamics of chemically reactive flows were extensively explored by [14], [15], and [16], who concentrated on the consequences of chemical reactions on fluid movement near oscillating plates and stretching surfaces across various scenarios, including heat and mass transfer, and the presence of magnetic fields. This paved the way for more nuanced studies, such as those by [17] and [18, 19], which investigated the unsteady flow near vertical plates with chemical reactions under thermal stratification. [20] extended these observations to porous media with a focus on mass diffusion, and [21] further broadened the scope by examining non-Newtonian fluids in porous media affected by chemical reaction and thermal stratification, highlighting the

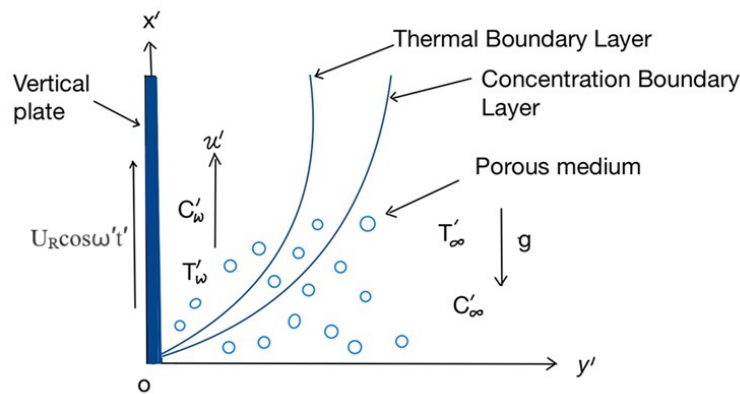


Figure 1. Physical Model and coordinate system

comprehensive exploration of these complex interactions in fluid dynamics.

This research, offering profound implications for industries like chemical manufacturing, polymer production, and crystal separation, encompasses a wide array of studies on MHD unsteady and transient heat transfer in vertical plates. These studies, covering stratification, chemical reaction, magnetic field, porous medium, and radiation, collectively deepen our understanding of natural convection under diverse fluid and environmental conditions.

## 2. MATHEMATICAL ANALYSIS

Consider the problem of an unsteady Magnetohydrodynamic (MHD) flow of a viscous, incompressible, and stratified fluid over a vertically oscillating plate embedded in a porous medium. This setup is described using a rectangular Cartesian coordinate system  $(x', y', t')$ , where the  $y'$  axis is perpendicular to the plate and the  $x'$  axis is aligned vertically along the plate. The fluid velocity at any point  $(x', y', t')$  is denoted by  $q = (u', 0)$ . Initially, at  $t' = 0$ , both the temperature and concentration of the fluid at the plate are  $T'_\infty$  and  $C'_\infty$ , respectively. For times  $t' > 0$ , the plate starts oscillating in its own plane with a velocity of  $U_R \cos \omega t'$  relative to the gravitational field. Concurrently, at  $t' > 0$ , the temperature at the plate rises to  $T'_w + (T'_w - T'_\infty)At'$ , and the concentration increases to  $C'_w + (C'_w - C'_\infty)e^{a't'}$ . These dynamics are analyzed under the assumption of the standard Boussinesq approximation, leading to the formulation of equations for motion, energy, and concentration, alongside the defined boundary conditions.

$$\frac{\partial u'}{\partial t'} = g\beta(T' - T'_\infty) + g\beta^*(C' - C'_\infty) + \nu \frac{\partial^2 u'}{\partial y'^2} - \frac{\sigma B_0^2 u'}{\rho} - \frac{\nu}{k} u' \tag{1}$$

$$\frac{\partial T'}{\partial t'} = \frac{k}{\rho C_p} \frac{\partial^2 T'}{\partial y'^2} - \gamma' u' \tag{2}$$

$$\frac{\partial C'}{\partial t'} = D \frac{\partial^2 C'}{\partial y'^2} - K'_c u' \tag{3}$$

with the following initial and boundary Conditions:

$$\begin{aligned} u' = 0 & & T' = T'_\infty & & C' = C'_\infty & & \forall y', t' \leq 0 \\ u' = U_R \cos \omega t' & & T' = T'_w + (T'_w - T'_\infty)At' & & C' = C'_w + (C'_w - C'_\infty)e^{a't'} & & \text{at } y' = 0, t' > 0 \\ u' \rightarrow 0 & & T' \rightarrow T'_\infty & & C' \rightarrow C'_\infty & & \text{as } y' \rightarrow \infty, t' > 0 \end{aligned}$$

where  $a'$ ,  $\eta$ ,  $\nu$ ,  $D$ , and  $Da$  are respectively constant, similarity parameter, kinematic viscosity, mass diffusion coefficient, darcy number. The "thermal stratification parameter" is termed as  $\gamma = \frac{dT'_\infty}{dx'} + \frac{g}{C_p}$ . The term "thermal stratification" refers to the combination of vertical temperature advection  $\left(\frac{dT'_\infty}{dx'}\right)$ , where the temperature of the surrounding fluid is height-dependent, and work of compression  $\left(\frac{g}{C_p}\right)$ , the rate at which particles in a fluid do reversible work due to compression.

and we provide non-dimensional quantities in the following:

$$U = \frac{u'}{U_R}, \quad t = \frac{t'}{t_R}, \quad y = \frac{y'}{L_R}, \quad \omega = \omega' t_R, \quad \theta = \frac{T' - T'_\infty}{T'_w - T'_\infty}, \quad C = \frac{C' - C'_\infty}{C'_w - C'_\infty}, \quad M = \frac{\sigma B_0^2 \nu}{\rho U_R^2}, \quad A = \frac{1}{t_R}$$

$$Gr = \frac{\nu g \beta (T'_w - T'_\infty)}{U_R^3}, \quad Gc = \frac{\nu g \beta^* (C'_w - C'_\infty)}{U_R^3}, \quad Pr = \frac{\mu C_p}{k}, \quad Sc = \frac{\nu}{D}, \quad a = a' t_R, \quad \Delta T = T'_w - T'_\infty,$$

$$Da = \frac{U_R^2 k'}{\nu^2}, \quad \gamma = \frac{\gamma' L_R}{\Delta T}, \quad K_c = \frac{K'_c L_R^2}{\nu}, \quad U_R = (\nu g \beta \Delta T)^{1/3}, \quad t_R = (g \beta \Delta T)^{-2/3} \nu^{1/3}, \quad L_R = \left( \frac{g \beta \Delta T}{\nu^2} \right)^{-1/3}$$

Where  $Pr$  is Prandtl number,  $Gr$  is thermal Grashof number,  $Gc$  is mass Grashof number,  $M$  is Magnetic parameter,  $Sc$  is Schmidt number,  $t$  is time in dimensionless coordinate,  $L_R$  is reference length,  $t_R$  is reference time,  $U$  is dimensionless velocity,  $U_R$  is reference velocity,  $\mu$  is viscosity of fluid,  $\theta$  is the dimensionless temperature,  $C$  is dimensionless concentration,  $\omega$  is frequency of oscillation. Then non-dimensional forms of the equations (1)-(3) are given by

$$\frac{\partial U}{\partial t} = Gr\theta + GcC + \frac{\partial^2 U}{\partial y^2} - \left( M + \frac{1}{Da} \right) U \tag{4}$$

$$\frac{\partial \theta}{\partial t} = \frac{1}{Pr} \frac{\partial^2 \theta}{\partial y^2} - \gamma U \tag{5}$$

$$\frac{\partial C}{\partial t} = \frac{1}{Sc} \frac{\partial^2 C}{\partial y^2} - K_c C \tag{6}$$

Non-dimensional forms of initial and boundary Conditions are:

$$\begin{array}{llll} U = 0 & \theta = 0 & C = 0 & \forall y, t \leq 0 \\ U = \cos \omega t & \theta = t & C = e^{at} & \text{at } y = 0, t > 0 \\ U \rightarrow 0 & \theta \rightarrow 0 & C \rightarrow 0 & \text{as } y \rightarrow \infty, t > 0 \end{array} \tag{7}$$

### 3. METHOD OF SOLUTION

We discovered that the Laplace transform method produces an equation of non-tractable form for any arbitrary Prandtl or Schmidt number. The non-dimensional governing equations (4)-(6) with boundary conditions (7), are solved for the tractable situation of  $Pr = 1, Sc = 1$ . Hence, the expressions for velocity, temperature, and concentration profiles can be determined with the help of [22] and [23] are as follows

$$\begin{aligned} U = & D_2 \frac{\eta}{t\sqrt{\pi}} e^{-Et-\eta^2} + D_3 f_1(E, -a) - \frac{E}{2(P-E)} [f_1(E, i\omega) + f_1(E, -i\omega)] + \frac{Gr}{P-E} f_2(E) + (D_1 - D_2) \\ & \frac{\eta}{t\sqrt{\pi}} e^{-Pt-\eta^2} + \frac{P}{2(P-E)} [f_1(P, i\omega) + f_1(P, -i\omega)] + (aD_1 + D_1K_c - D_3) f_1(P, -a) - \frac{Gr}{P-E} f_2(P) \\ & D_1(a + K_c) f_1(K_c, -a) \end{aligned} \tag{8}$$

$$\begin{aligned} \theta = & D_4 t \left\{ (1 + 2\eta^2) \operatorname{erfc}(\eta) - \frac{2\eta}{\sqrt{\pi}} e^{-\eta^2} \right\} - \gamma \left[ \left( D_2 + \frac{D_1 - D_2}{P} - \frac{D_1}{K_c} \right) \frac{\eta}{t\sqrt{\pi}} e^{-\eta^2} + \left\{ \frac{D_3}{E} + \frac{aD_1 + D_1K_c - D_3}{P} \right. \right. \\ & \left. \left. - \frac{D_1(a + K_c)}{K_c} \right\} f_3(a) - \frac{D_2}{E} \frac{\eta}{t\sqrt{\pi}} e^{-Et-\eta^2} - \frac{D_1 - D_2}{P} \frac{\eta}{t\sqrt{\pi}} e^{-Pt-\eta^2} + \frac{D_1}{K_c} \frac{\eta}{t\sqrt{\pi}} e^{-K_c t - \eta^2} - \frac{D_3}{E} f_1(E, -a) \right. \\ & \left. - \frac{Gr}{E(P-E)} f_2(E) + \frac{1}{2(P-E)} (f_1(E, i\omega) + f_1(E, -i\omega)) - \frac{1}{2(P-E)} (f_1(P, i\omega) + f_1(P, -i\omega)) \right. \\ & \left. + \frac{aD_1 + D_1K_c - D_3}{P} f_1(P, -a) + \frac{D_1(a + K_c)}{K_c} f_1(K_c, -a) + \frac{Gr}{P(P-E)} f_2(p) \right] \end{aligned} \tag{9}$$

$$C = \frac{1}{2} \left[ e^{-2\eta\sqrt{(a+K_c)t}} \operatorname{erfc}(\eta - \sqrt{(a+K_c)t}) + e^{2\eta\sqrt{(a+K_c)t}} \operatorname{erfc}(\eta + \sqrt{(a+K_c)t}) \right] \tag{10}$$

Where,

$$\eta = \frac{y}{2\sqrt{t}}, \quad EP = \gamma Gr, \quad E + P = M + \frac{1}{Da}, \quad E - P = \sqrt{\left(M + \frac{1}{Da}\right)^2 - 4\gamma Gr}$$

$$D_1 = \frac{Gc}{K_c \left(K_c - M - \frac{1}{Da}\right) + \gamma Gr}, \quad D_2 = \frac{4aD_1 - D_1K_c + D_1P}{P - E}$$

$$D_3 = \frac{a^2D_1 + aD_1K_c + aD_1P + D_1K_cP + 3a^2D_1 - 2aD_1K_c - D_1K_c^2 + Gc}{P - E}, \quad D_4 = 1 + \frac{\gamma Gr}{P(P - E)} - \frac{\gamma Gr}{E(P - E)}$$

Also,  $f_i$ 's are inverse Laplace's transforms given by

$$f_1(p, q) = L^{-1} \left\{ \frac{e^{-y\sqrt{s+p}}}{s + q} \right\}, \quad f_2(p) = L^{-1} \left\{ \frac{e^{-y\sqrt{s+p}}}{s^2} \right\}, \quad f_3(q) = L^{-1} \left\{ \frac{e^{-y\sqrt{s}}}{s + q} \right\}$$

We separate the complex arguments of the error function contained in the previous expressions into real and imaginary parts using the formulas provided by [22].

#### 4. CLASSICAL CASE ( $\gamma = 0$ )

We derived solutions for the classical case of no thermal stratification ( $\gamma = 0$ ). We want to compare the results of the fluid with thermal stratification to the case with no stratification. Hence, the solutions for the classical case with boundary conditions (7) by using the Laplace transformation are as follows:

$$\theta_c = (1 + 2\eta^2)erfc(\eta) - \frac{2\eta}{\sqrt{\pi}}e^{-\eta^2} \tag{11}$$

$$U_c = \frac{1}{2} [f_1((E + P), i\omega) + f_1((E + P), -i\omega)] - \frac{Gr}{E + P}f_2(E + P) + \frac{Gc}{K_c - (E + P)}f_1((E + P), -a) + \frac{tGr}{(E + P)} \left\{ (1 + 2\eta^2)erfc(\eta) - \frac{2\eta}{\sqrt{\pi}}e^{-\eta^2} \right\} - \frac{Gc}{K_c - (E + P)}f_1(K_c, -a) \tag{12}$$

##### 4.1. Skin-Friction

The non-dimensional Skin-Friction, which is determined as shear stress on the surface, is obtained by

$$\tau = -\frac{dU}{dy} \Big|_{y=0}$$

The solution for the Skin-Friction is calculated from the solution of Velocity profile  $U$ , represented by (8), as follows:

$$\begin{aligned} \tau = & \frac{D_2e^{-Et}}{2\sqrt{\pi t^3}} + \frac{(D_1 - D_2)e^{-Pt}}{2\sqrt{\pi t^3}} + D_3 \left[ e^{at}\sqrt{a + E} \operatorname{erf}(\sqrt{(a + E)t}) + \frac{e^{-Et}}{\sqrt{\pi t}} \right] - \frac{E}{2(P - E)} \\ & \left[ e^{i\omega t}\sqrt{E + i\omega} \operatorname{erf}(\sqrt{(E + i\omega)t}) + e^{-i\omega t}\sqrt{E - i\omega} \operatorname{erf}(\sqrt{(E - i\omega)t}) + \frac{2e^{-Et}}{\sqrt{\pi t}} \right] + \frac{Gr}{P - E} \\ & \left[ t\sqrt{E} \operatorname{erf}(\sqrt{Et}) - t\sqrt{P} \operatorname{erf}(\sqrt{Pt}) + \sqrt{\frac{t}{\pi}}(e^{-Et} - e^{-Pt}) + \frac{\operatorname{erf}(\sqrt{Et})}{2\sqrt{E}} - \frac{\operatorname{erf}(\sqrt{Pt})}{2\sqrt{P}} \right] \\ & (aD_1 + D_1K_c - D_3) \left[ e^{at}\sqrt{a + P} \operatorname{erf}(\sqrt{(a + P)t}) + \frac{e^{-Pt}}{\sqrt{\pi t}} \right] + \frac{P}{2(P - E)} \\ & \left[ e^{i\omega t}\sqrt{P + i\omega} \operatorname{erf}(\sqrt{(P + i\omega)t}) + e^{-i\omega t}\sqrt{P - i\omega} \operatorname{erf}(\sqrt{(P - i\omega)t}) + \frac{2e^{-Pt}}{\sqrt{\pi t}} \right] \\ & - D_1K_c \left[ e^{at}\sqrt{a + K_c} \operatorname{erf}(\sqrt{(a + K_c)t}) + \frac{e^{-K_c t}}{\sqrt{\pi t}} \right] - (D_1 + aD_1) \frac{e^{K_c t}}{2\sqrt{\pi t^3}} \end{aligned}$$

The solution for the Skin-Friction for the classical case is given from the expression (12), which is represented by

$$\begin{aligned} \tau^* = & \left[ e^{i\omega t} \sqrt{(E+P) + i\omega} \operatorname{erf} \left( \sqrt{(E+P)t + i\omega t} \right) + e^{-i\omega t} \sqrt{(E+P) - i\omega} \operatorname{erf} \left( \sqrt{(E+P)t - i\omega t} \right) \right. \\ & \left. + \frac{2e^{-(E+P)t}}{\sqrt{\pi t}} \right] - \frac{Gr}{(E+P)} \left[ t\sqrt{(E+P)} \operatorname{erf} \left( \sqrt{(E+P)t} \right) + \sqrt{\frac{t}{\pi}} e^{-(E+P)t} + \frac{\operatorname{erf}(\sqrt{(E+P)t})}{2\sqrt{(E+P)}} \right] \\ & + \frac{Gc}{K_c - (E+P)} \left[ e^{at} \sqrt{(E+P) + a} \operatorname{erf} \left( \sqrt{(E+P)t + at} \right) + \frac{e^{-(E+P)t}}{\sqrt{\pi t}} \right] + \sqrt{\frac{t}{\pi}} \frac{2Gr}{(E+P)} \\ & - \frac{Gc}{K_c - (E+P)} \left[ e^{at} \sqrt{K_c + a} \operatorname{erf} \left( \sqrt{(K_c + a)t} \right) + \frac{e^{-K_c t}}{\sqrt{\pi t}} \right] \end{aligned}$$

### 4.2. Nusselt Number

The non-dimensional Nusselt number, which is determined as the rate of heat transfer, is obtained by

$$Nu = - \left. \frac{d\theta}{dy} \right|_{y=0}$$

The solution for the Nusselt number is calculated from the solution of Temperature profile  $\theta$ , represented by (9), as follows:

$$\begin{aligned} Nu = & 2D_4 \sqrt{\frac{t}{\pi}} - \gamma \left[ \frac{D_2}{2E\sqrt{\pi t^3}} + \left\{ \frac{D_3}{E} + \frac{aD_1 - D_1K_c - D_3}{P} - \frac{D_1(a + K_c)}{K_c} \right\} \left\{ e^{at} \sqrt{a} \operatorname{erf}(\sqrt{at}) + \frac{1}{\sqrt{\pi t}} \right\} \right. \\ & + \frac{D_1 - D_2}{2P\sqrt{\pi t^3}} - \frac{D_1}{2K_c\sqrt{\pi t^3}} - \frac{D_2 e^{-Et}}{2\sqrt{\pi t^3}} - \frac{D_3}{E} \left\{ e^{at} \sqrt{a + E} \operatorname{erf} \left( \sqrt{(a + E)t} \right) + \frac{e^{-Et}}{\sqrt{\pi t}} \right\} - \frac{Gr}{E(P - E)} \\ & \left. \left\{ t\sqrt{E} \operatorname{erf}(\sqrt{Et}) + \sqrt{\frac{t}{\pi}} e^{-Et} + \frac{\operatorname{erf}(\sqrt{Et})}{2\sqrt{E}} \right\} - \frac{(D_1 - D_2)e^{-Pt}}{2\sqrt{\pi t^3}} + \frac{1}{2(P - E)} \right. \\ & \left. \left\{ e^{i\omega t} \sqrt{E + i\omega} \operatorname{erf}(\sqrt{(E + i\omega)t}) + e^{-i\omega t} \sqrt{E - i\omega} \operatorname{erf}(\sqrt{(E - i\omega)t}) + \frac{2e^{-Et}}{\sqrt{\pi t}} \right\} - \frac{1}{2(P - E)} \right. \\ & \left. \left\{ e^{i\omega t} \sqrt{P + i\omega} \operatorname{erf}(\sqrt{(P + i\omega)t}) + e^{-i\omega t} \sqrt{P - i\omega} \operatorname{erf}(\sqrt{(P - i\omega)t}) + \frac{2e^{-Pt}}{\sqrt{\pi t}} \right\} - \frac{aD_1 - D_1K_c - D_3}{P} \right. \\ & \left. \left\{ e^{at} \sqrt{a + P} \operatorname{erf}(\sqrt{(a + P)t}) + \frac{e^{-Pt}}{\sqrt{\pi t}} \right\} + \frac{D_1 e^{-K_c t}}{2K_c\sqrt{\pi t^3}} + \frac{D_1(a + K_c)}{K_c} \left\{ e^{at} \sqrt{a + K_c} \operatorname{erf}(\sqrt{(a + K_c)t}) \right. \right. \\ & \left. \left. + \frac{e^{-K_c t}}{\sqrt{\pi t}} \right\} + \frac{Gr}{P(P - E)} \left\{ t\sqrt{P} \operatorname{erf}(\sqrt{Pt}) + \sqrt{\frac{t}{\pi}} e^{-Pt} + \frac{\operatorname{erf}(\sqrt{Pt})}{2\sqrt{P}} \right\} \right] \end{aligned}$$

The solution for the Nusselt number for the classical case is given from the expression (11), which is represented by

$$Nu^* = 2 \sqrt{\frac{t}{\pi}}$$

### 4.3. Sherwood Number

The non-dimensional Sherwood number, which is determined as the rate of mass transfer, is obtained by

$$Sh = - \left. \frac{dC}{dy} \right|_{y=0}$$

The solution for the Sherwood number is calculated from the solution of Concentration profile  $C$ , represented by (10), as follows:

$$Sh = \sqrt{a + K_c} \operatorname{erf}(\sqrt{(a + K_c)t}) + \frac{1}{\sqrt{\pi t}} e^{-(a+K_c)t}$$

### 5. RESULT AND DISCUSSIONS

We calculated the numerical values for velocity, temperature, concentration, skin friction, Nusselt number, and Sherwood number by utilizing the solutions obtained in previous sections, for different values of the physical parameters  $\gamma, Gr, Gc, M, Da, K_c, \omega$ , and  $t$ . This process enhanced our comprehension of the problem's physical importance. Additionally, by employing MATLAB, we visually represented these calculations in Figures 2 through 17.

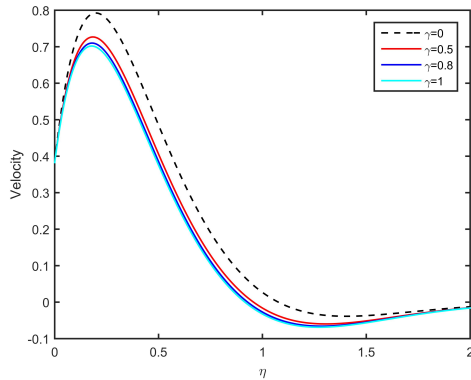


**Figure 2.** Effects of  $\gamma$  on Velocity Profile for  $t = 1.5, a = 0.2, \omega = \pi/4, Gr = 5, Gc = 5, M = 2, Da = 0.5, K_c = 0.2$

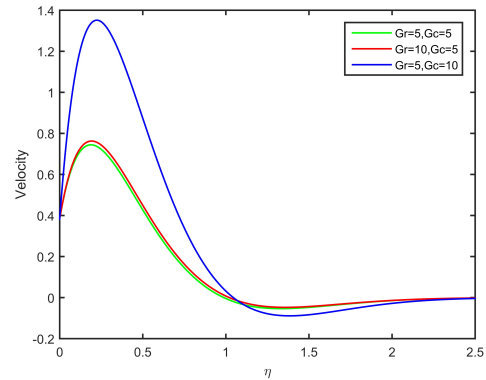


**Figure 3.** Effects of  $\gamma$  on Velocity Profile for  $t = 1.5, a = 0.2, \omega = \pi/4, \gamma = 0.5, M = 2, Da = 0.5, K_c = 0.2$

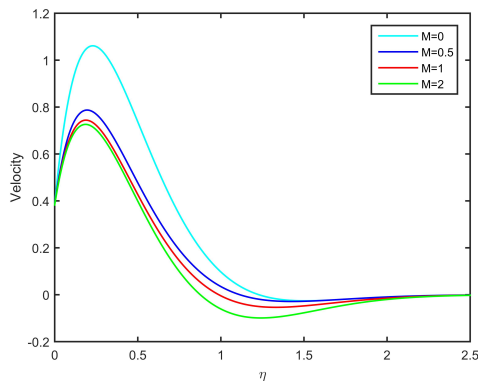


**Figure 4.** Effects of  $M$  on Velocity Profile for  $t = 1.5, a = 0.2, \omega = \pi/4, Gr = 5, Gc = 5, \gamma = 0.5, Da = 0.5, K_c = 0.2$

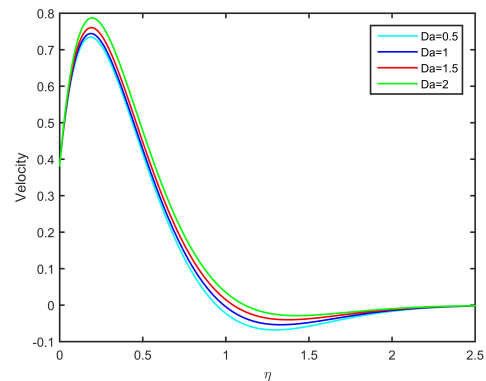


**Figure 5.** Effects of  $Da$  on Velocity Profile for  $t = 1.5, a = 0.2, \omega = \pi/4, Gr = 5, Gc = 5, \gamma = 0.5, M = 2, K_c = 0.2$

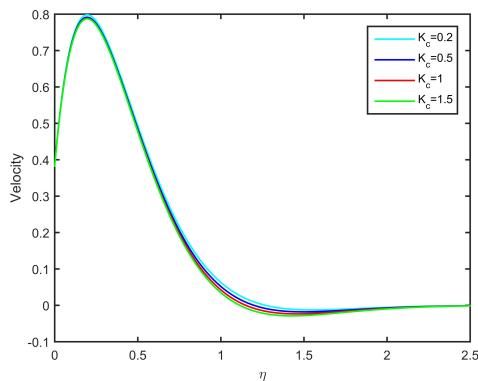


**Figure 6.** Effects of  $K_c$  on Velocity Profile for  $t = 1.5, a = 0.2, \omega = \pi/4, Gr = 5, Gc = 5, \gamma = 0.5, M = 2, Da = 0.5$

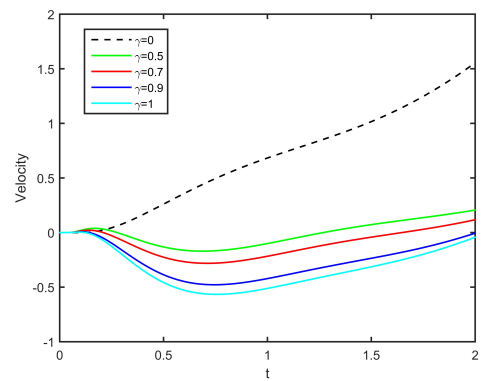


**Figure 7.** Effects of  $\gamma$  on Velocity Profile against time for  $y = 1.2, a = 0.2, \omega = \pi/4, Gr = 5, Gc = 5, \gamma = 0.5, M = 2, Da = 0.5$

The presented Figures 2 through 7 illustrate the influence of various physical parameters on velocity profiles. In Figure 2, as the parameter  $\gamma$  increases, there's a marked reduction in peak velocity, suggesting a damping

effect. In the 3 and 4 Figures, it is evident that increases in Grashof number  $Gr$  for thermal buoyancy and magnetic parameter  $M$  cause velocity profiles to peak at lower values and shift to the left. Figure 5 indicates that with increasing Darcy number  $Da$ , peak velocities increase, suggesting less resistance to flow through porous media. Figure 6 highlights the influence of the chemical reaction parameter  $K_c$ , with higher values leading to lower velocities, indicative of the retarding influence of the chemical reaction on the flow. Lastly, Figure 7 shows that as the thermal stratification parameter ( $\gamma$ ) increases, the fluid's velocity initially decreases and then stabilizes over time, with ( $\gamma = 0$ ) exhibiting the highest velocity.

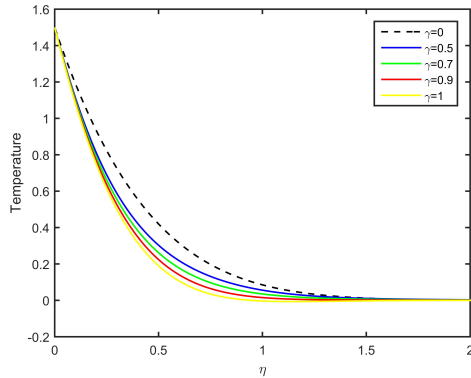


**Figure 8.** Effects of  $\gamma$  on Temperature Profile for  $t = 1.5, a = 0.2, \omega = \pi/4, Gr = 5, Gc = 5, M = 2, Da = 0.5, K_c = 0.2$

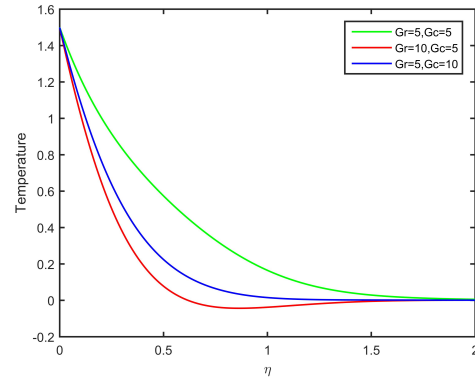


**Figure 9.** Effects of  $\gamma$  on Temperature Profile for  $t = 1.5, a = 0.2, \omega = \pi/4, \gamma = 0.5, M = 2, Da = 0.5, K_c = 0.2$

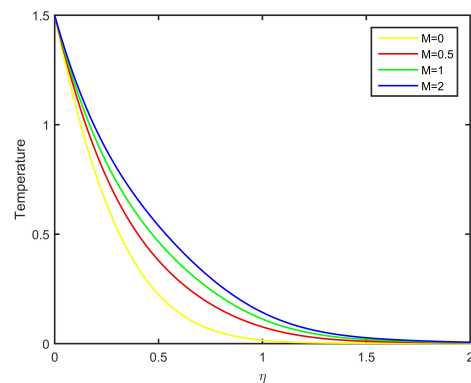


**Figure 10.** Effects of  $M$  on Temperature Profile for  $t = 1.5, a = 0.2, \omega = \pi/4, Gr = 5, Gc = 5, \gamma = 0.5, Da = 0.5, K_c = 0.2$

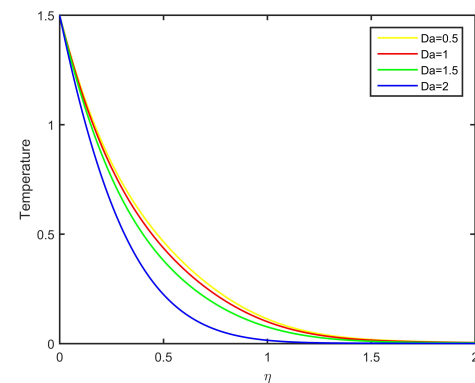


**Figure 11.** Effects of  $Da$  on Temperature Profile for  $t = 1.5, a = 0.2, \omega = \pi/4, Gr = 5, Gc = 5, \gamma = 0.5, M = 2, K_c = 0.2$

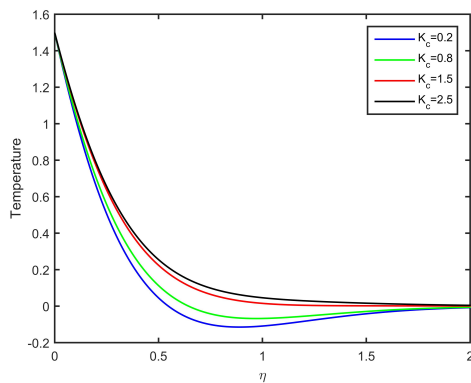


**Figure 12.** Effects of  $K_c$  on Temperature Profile for  $t = 1.5, a = 0.2, \omega = \pi/4, Gr = 5, Gc = 5, \gamma = 0.5, M = 2, Da = 0.5$

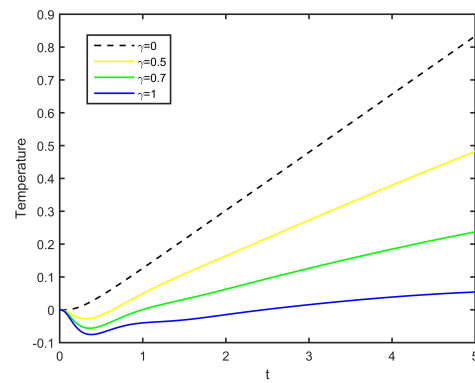


**Figure 13.** Effects of  $\gamma$  on Temperature Profile against time for  $y = 1.2, a = 0.2, \omega = \pi/4, Gr = 5, Gc = 5, \gamma = 0.5, M = 2, Da = 0.5$

Figures 8 through 13 depicts the temperature profiles for various physical parameters. In figure 8 shows that

as the parameter  $\gamma$  increases, the temperature decreases across the profile, with the steepest gradient near  $\gamma = 0$ . Figure 9 indicates that higher Grashof numbers for thermal buoyancy lead to lower temperatures, particularly noticeable for  $Gr = 10, Gc = 5$ . Figure 10 suggests that an increase in the magnetic parameter  $M$  results in a more uniform temperature distribution, highlighting magnetic damping of thermal fluctuations. In Fig 11, higher Darcy numbers result in lower temperatures, indicating reduced resistance to thermal conduction in porous media. Figure 12 shows that reduced chemical reaction parameters  $K_c$  correspond to lower temperatures. Finally, fig 13 demonstrates the time evolution of the temperature profile, with higher  $\gamma$  values leading to a slower increase in temperature over time, likely due to thermal diffusion or delayed thermal response in the system.

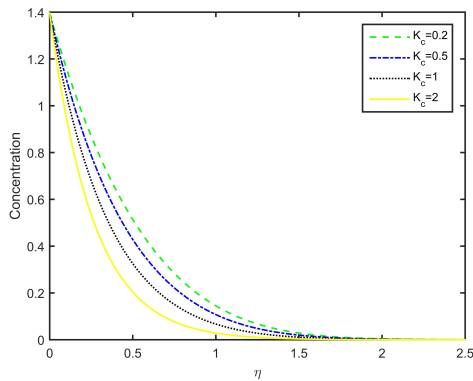


**Figure 14.** Effects of  $K_c$  on Concentration Profile for  $t = 1.6, a = 0.2$

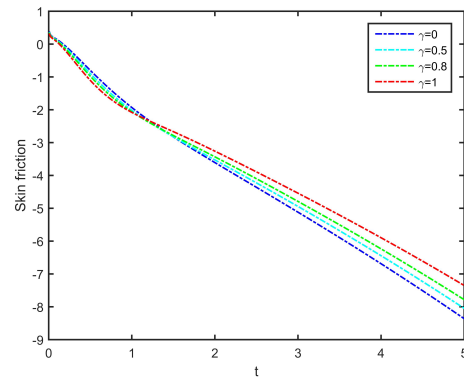


**Figure 15.** Effects of  $\gamma$  on Skin friction for  $a = 0.2, \omega = \pi/4, Gr = 5, Gc = 5, M = 2, Da = 0.5, K_c = 0.2$

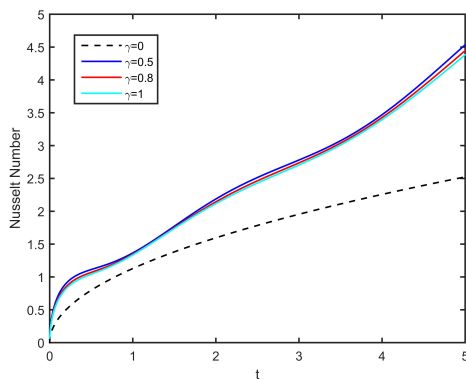


**Figure 16.** Effects of  $\gamma$  on Nusselt Number for  $a = 0.2, \omega = \pi/4, Gr = 5, Gc = 5, M = 2, Da = 0.5, K_c = 0.2$

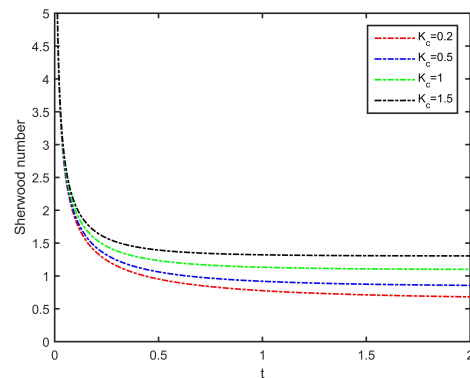


**Figure 17.** Effects of  $K_c$  on Sherwood Number for  $t = 1.6, a = 0.2$

Figure 14 displays concentration profiles for different values of the chemical reaction parameter  $K_c$ . As  $K_c$  increases, concentration within the boundary layer decreases, indicating a stronger chemical reaction diminishes species concentration.

Figure 15 presents skin friction decreasing linearly over time for different values of  $\gamma$ , with the rate of decrease being similar across the values. Nusselt number increases linearly over time for different values of  $\gamma$ , with higher  $\gamma$ , having a steeper slope as shown in figure 16. Figure 17 illustrates the Sherwood number decreasing with time and approaching a constant value for various  $K_c$ , with higher  $K_c$  resulting in a lower asymptote.

### 6. CONCLUSION

Building on the insights garnered from the discussion earlier in this paper, the subsequent sections outline the key conclusions drawn from this research.


- As  $\gamma$  increases, both velocity and temperature decrease due to the stabilizing influence of thermal stratification, leading the fluid towards a steady state. Conversely, in the classical scenario without thermal



stratification, the velocity and temperature remain higher compared to those in the thermally stratified fluid.

- As  $Gr$  and  $Gc$  rise, velocity increases, yet temperature falls with the increase of  $Gr$  and  $Gc$ . Conversely, an increase in  $M$  leads to a decrease in velocity while causing an increase in temperature.
- As the Darcy number  $Da$  increases, there is an increase in velocity, whereas the temperature decreases with the rise of  $Da$ .
- With an increase in the chemical reaction parameter  $K_c$ , both velocity and concentration decrease, while the temperature increases as  $K_c$  rises.
- In the isothermal scenario, there is a reduction in both Skin friction and Nusselt numbers when compared to the stratification scenario.

### ORCID

 **Digbash Sahu**, <https://orcid.org/0009-0005-8925-2048>; 
  **Rudra Kanta Deka**, <https://orcid.org/0009-0007-1573-4890>

### REFERENCES

- [1] R. Siegel, "Transient free convection from a vertical flat plate," Transactions of the American Society of Mechanical Engineers, **80**(2), 347-357 (1958). <https://doi.org/10.1115/1.4012369>.
- [2] E.R. Menold, and K.T. Yang, "Asymptotic solutions for unsteady laminar free convection on a vertical plate," Trans ASME: J. Appl. Mech., **29**, 124-126 (1962). <http://doi.org/10.1115/1.3636443>.
- [3] J.A. Schetz, and R. Eichhorn, "Unsteady natural convection in the vicinity of a doubly infinite vertical plate," Trans ASME C: J. Heat Transfer, **84**(4), 334-338 (1962). <https://doi.org/10.1115/1.3684386>
- [4] U.N. Das, R.K. Deka, and V.M. Soundalgekar, "Transient free convection flow past an infinite vertical plate with periodic temperature variation," J. Heat Transfer, **121**(4), 1091-1094 (1999). <https://doi.org/10.1115/1.2826063>
- [5] J.S. Park, and J.M. Hyun, "Technical Note Transient behavior of vertical buoyancy layer in a stratified fluid," International journal of heat and mass transfer, **41**(24), 4393-4397 (1998). [https://doi.org/10.1016/S0017-9310\(98\)00175-6](https://doi.org/10.1016/S0017-9310(98)00175-6)
- [6] J.S. Park, "Transient buoyant flows of a stratified fluid in a vertical channel," KSME international journal, **15**, 656-664 (2001). <http://doi.org/10.1007/bf03184382>
- [7] A. Shapiro, and E. Fedorovich, "Unsteady convectively driven flow along a vertical plate immersed in a stably stratified fluid," Journal of Fluid Mechanics, **498**, 333-352 (2004). <https://doi.org/10.1017/S0022112003006803>
- [8] E. Magyari, I. Pop, and B. Keller, "Unsteady free convection along an infinite vertical flat plate embedded in a stably stratified fluid-saturated porous medium," Transport in porous media, **62**, 233-249 (2006). <https://doi.org/10.1007/s11242-005-1292-6>
- [9] R.C. Chaudhary, and A. Jain, "MHD heat and mass diffusion flow by natural convection past a surface embedded in a porous medium," Theoretical and Applied Mechanics, **36**(1), 1-27 (2009). <https://doi.org/10.2298/TAM0901001C>
- [10] Y.D. Reddy, B.S. Goud, and M.A. Kumar, "Radiation and heat absorption effects on an unsteady MHD boundary layer flow along an accelerated infinite vertical plate with ramped plate temperature in the existence of slip condition," Partial Differential Equations in Applied Mathematics, **4**, 100166 (2021). <https://doi.org/10.1016/j.padiff.2021.100166>
- [11] G.V.R. Reddy, C.V.R. Murthy, and N.B. Reddy, "Unsteady MHD free convective mass transfer flow past an infinite vertical porous plate with variable suction and Soret effect," Int. J. of Appl. Math. and Mech. **7**(21), 70-84 (2011).
- [12] R. Muthucumaraswamy, and P. Sivakumar, "Hydro magnetic effects on parabolic flow past an infinite isothermal vertical plate with variable mass diffusion in the presence of thermal radiation and chemical reaction," International Journal of Recent Technology and Engineering, **4**(2), 5-10 (2015). <https://doi.org/10.1515/ijame-2016-0006>
- [13] F.M.N. El-Fayez, "Effects of chemical reaction on the unsteady free convection flow past an infinite vertical permeable moving plate with variable temperature," Journal of surface engineered materials and advanced technology, **2**(2), 100- 109 (2012). <http://dx.doi.org/10.4236/jsemat.2012.22016>
- [14] A. Bhattacharya, and R.K. Deka, "Theoretical study of chemical reaction effects on vertical oscillating plate immersed in a stably stratified fluid," Research Journal of Applied Sciences, Engineering and Technology, **3**(9), 887-898 (2011). <https://maxwellsci.com/print/rjaset/v3-887-898.pdf>
- [15] U.N. Das, R. Deka, and V.M. Soundalgekar, "Effects of mass transfer on flow past an impulsively started infinite vertical plate with constant heat flux and chemical reaction," Forschung im Ingenieurwesen, **60**(10), 284-287 (1994). <https://doi.org/10.1007/BF02601318>
- [16] R. Kandasamy, K. Periasamy, and K.K.S. Prabhu, "Chemical reaction, heat and mass transfer on mhd flow over a vertical stretching surface with heat source and thermal stratification effects," International Journal of Heat and Mass Transfer, **48**(21-22), 4557-4561 (2005). <https://doi.org/10.1016/j.ijheatmasstransfer.2005.05.006>

- [17] N. Kalita, R.K. Deka, and R.S. Nath, "Unsteady Flow Past an Accelerated Vertical Plate with Variable Temperature in Presence of Thermal Stratification and Chemical Reaction," East European Journal of Physics, (3), 441-450 (2023). <https://doi.org/10.26565/2312-4334-2023-3-49>
- [18] R. S. Nath, and R.K. Deka, "The Effects of Thermal Stratification on Flow Past an Infinite Vertical Plate in Presence of Chemical Reaction," East European Journal of Physics, (3), 223-232 (2023). <https://doi.org/10.26565/2312-4334-2023-3-19>
- [19] R.S. Nath, R.K. Deka, and H. Kumar, "The Effect of Thermal Stratification on Unsteady Parabolic Flow Past An Infinite Vertical Plate With Chemical Reaction," East European Journal of Physics, (4), 77-86 (2023). <https://doi.org/10.26565/2312-4334-2023-4-08>
- [20] H. Kumar, and R.K. Deka, "Thermal and Mass Stratification Effects on Unsteady Flow Past an Accelerated Infinite Vertical Plate with Variable Temperature and Exponential Mass Diffusion in Porous Medium," East European Journal of Physics, (4), 87-97 (2023). <https://doi.org/10.26565/2312-4334-2023-4-09>
- [21] A.M. Megahed, and W. Abbas, "Non-newtonian cross fluid flow through a porous medium with regard to the effect of chemical reaction and thermal stratification phenomenon," Case Studies in Thermal Engineering, **29**, 101715 (2022). <https://doi.org/10.1016/j.csite.2021.101715>
- [22] Abramowitz, Milton, I.A. Stegun, and R.H. Romer, "Handbook of mathematical functions with formulas, graphs, and mathematical tables," American Journal of Physics, **56**(10), 958 (1988). <https://doi.org/10.1119/1.15378>
- [23] R.B. Hetnarski, "An algorithm for generating some inverse Laplace transforms of exponential form," Zeitschrift für angewandte Mathematik und Physik ZAMP, **26**, 249-253 (1975). <https://doi.org/10.1007/bf01591514>

## ВПЛИВ ТЕРМІЧНОЇ СТРАТИФІКАЦІЇ ТА ХІМІЧНОЇ РЕАКЦІЇ НА МГД-ПОТІК ЧЕРЕЗ КОЛИВАЛЬНУ ВЕРТИКАЛЬНУ ПЛАСТИНУ В ПОРИСТОМУ СЕРЕДОВИЩІ ЗІ ЗМІНОЮ ТЕМПЕРАТУРИ ТА ЕКСПОНЕНЦІАЛЬНОЮ ДИФУЗІЄЮ МАСИ

Дігбаш Саху, Рудра Канта Дека

*Факультет математики, Університет Гаухаті, Гувахаті, 781014, Ассам, Індія*

У цій роботі досліджується термічна стратифікація та вплив хімічної реакції на МГД-потік через коливальну вертикальну пластину в пористому середовищі зі зміною температури та експоненціальною масовою дифузією. Завдяки застосуванню методу перетворення Лапласа в статті отримано аналітичні рішення, які точно відображають фізичну динаміку потоку. Розслідування використовує складні математичні моделі для ретельного вивчення складної динаміки між магнітогідродинамікою (МГД) і конвективними рухами, враховуючи низку умов, що включають температурні коливання та експоненціальну швидкість дифузії маси. Ключовим висновком цього дослідження є детальне порівняння результатів термічної стратифікації та тих, що спостерігаються в середовищах, де така стратифікація відсутня. Помічено, що реалізація стратифікації всередині потоку призводить до більш швидкого досягнення рівноважних або стаціонарних умов.

**Ключові слова:** МГД потік; хімічна реакція; термічна стратифікація; пористе середовище; коливальна вертикальна пластина; перетворення Лапласа; Matlab